

New Approaches for the Ethanol Oxidation Reaction of Pt/C on Carbon Cloth Using ATR-FTIR

R. F. B. De Souza¹, J. C. M. Silva¹, F. C. Simões¹, M. L. Calegari², A. O. Neto³, M. C. Santos^{1,*}

¹ Laboratório de Eletroquímica e Materiais Nanoestruturados, LEMN – CCNH - Centro de Ciências Naturais e Humanas, UFABC - Universidade Federal do ABC, CEP 09.210-170, Rua Santa Adélia 166, Bairro Bangu, Santo André, SP, Brazil.

² Grupo de Materiais Eletroquímicos e Métodos Eletroanalíticos, Instituto de Química de São Carlos, Universidade de São Paulo, Caixa Postal 780, 13566-590 São Carlos, SP, Brazil.

³ Instituto de Pesquisas Energéticas e Nucleares, IPEN, CNEN/SP, Av. Prof. Lineu Prestes, 2242 Cidade Universitária, CEP 05508-900, São Paulo, SP, Brazil

*E-mail: mauro.santos@ufabc.edu.br

Received: 4 Aril 2012 / Accepted: 11 May 2012 / Published: 1 June 2012

This work describes the study of the ethanol oxidation reaction of a Pt/C Etek electrocatalyst that was supported on different substrates, such as gold, glassy carbon and carbon cloth treated with PTFE. In the ethanol oxidation reaction, the activity varies with the substrate, as well as the pathways for ethanol oxidation, as studied by an ATR-FTIR *in situ* setup using the carbon cloth as the electrocatalyst support. The electrocatalyst Pt/C supported on gold starts acetaldehyde production from ethanol oxidation at an onset potential of 0.1 V less than that observed for the same process on Teflon-treated carbon cloth. The Pt/C supported on the carbon cloth starts its CO₂ production for the same oxidation process at 0.2 V less than on the Pt/C supported on gold substrate. The differences in catalytic activity for the ethanol oxidation reaction depend not only on the electrocatalyst but also on various electrode factors, such as the substrate, the roughness of the electrode and the charge transfer resistance.

Keywords: ethanol oxidation reaction, electrocatalysis, ATR-FTIR, roughness, Teflon-treated carbon cloth.

1. INTRODUCTION

The electrochemical oxidation of ethanol on Pt electrodes has been a subject of permanent interest for the development of fuel cell devices [1-3]. The use of ethanol in this context is attractive, due to its less toxic compared with methanol and also because it is produced from renewable sources

[3]. Ethanol is the smallest alcohol molecule that possesses a C–C bond. The strength of this bond makes it extremely stable and, therefore, difficult to break. As a result, the complete oxidation of compounds with C–C bonds is a great challenge in electrocatalysis. The partial oxidation of ethanol leads to the formation of acetaldehyde and acetic acid, which are compounds that cause a decrease in the electrical cell efficiency [4]. Moreover, the ethanol oxidation reaction pathway leads to the formation of strongly adsorbed intermediates which “poison” the platinum surface at low potentials [5]. Therefore, the efficiency for the ethanol electro-oxidation can be improved by both the development of more selective catalysts toward the CO₂ formation and by minimizing the catalyst poisoning at low potentials [6].

In recent decades, many studies have investigated the use of *in situ* FTIR spectroscopy for the oxidation of small organic molecules, such as ethanol, for fuel-cell purposes [7-9]. FTIR spectroscopy contributes to understanding the effects of the surface structure on the rate of reaction and provides an understanding into the nature of the interactions between organic molecules and the electrode surfaces. Thus, the mechanistic pathways of various surface reactions can be elucidated, and the oxidation kinetics of several organic molecules can be analyzed [5, 9, 10].

The *in situ* Fourier transformed infrared (FTIR) spectroscopy measurements can be carried out using different techniques. One technique is reflection-absorption spectroscopy (FTIR-RAS), which is used for the study of products and adsorbents [4, 11-16] and can be used for measurements with carbon dispersed electrocatalysts. However, limitations of this technique include mass transport and reactant depletion, as cited by Chen *et al.* [17], thereby making the IR spectrum more susceptible to the appearance of artifacts. Additionally, the use of reflective substrates, such as gold, are necessary [18].

Another technique involving *in situ* FTIR is the surface enhanced infrared absorption spectroscopy (SEIRAS). The configuration for this system is a prism–metal–solution. This powerful technique has been used to study adsorbents in metal films [19, 20]. In these measurements, a high surface sensitivity of ATR-FTIRS is used, and the technique allows the use of a bulk electrolyte, which largely reduces artifacts resulting from mass transport limitations and reactant depletion [17]. In contrast, this technique detects only adsorbents.

Most of the *in situ* FTIR studies described above are conducted under conditions that are inconsistent with those in direct alcohol fuel cells (DAFC). Understanding the mechanism of the ethanol oxidation reaction (EOR) that occurs in the fuel cell devices represents an important step toward improving the performance of the reaction and supports the EOR interpretation regarding the direct alcohol fuel cell operation.

In a DAFC, the electrocatalyst is supported on carbon paper or carbon cloth that is in contact with a proton exchange membrane. This support works as a gas diffusion layer (GDL) [21, 22], and it should be hydrophobic and provide passages for gas or liquid transport from the flow fields to the catalyst layers and water removal from the catalyst layers to the flow fields.

The carbon cloth was used in the electrochemical experiments to support the electrocatalysts for methanol and CO oxidation [23, 24]. However, FTIR-RAS and FTIR-SEIRAS were not appropriate techniques to perform measurements for the carbon cloth-supported electrocatalysts, as their surfaces are rough and non-reflective.

Attenuated Total Reflection (ATR) Spectroscopy uses a high refractive index crystal, thereby permitting radiation to reflect in the crystal one or more times, independent of the sample reflectance [25, 26], as a carbon [27], ceramics [28, 29] and biofilms [30, 31]. The IR beam interacts with the sample by means of an evanescent wave that penetrates into the sample that is in contact with the crystal and produces a spectrum [25, 26]. In this work, the electrochemical system is similar to the RAS on the surface of an ATR accessory, for this reason it can be possible make measurements *in situ* without the need for a reflective surface, as it has been done in our recent work [32].

The aim of this work is to use ATR-FTIR *in situ* spectroscopy adapted by our group [32] to study the electrochemical experiments of Pt/C supported on carbon cloth for ethanol oxidation. This system's electrodes are both non-reflective and rough, and, therefore, the ATR-FTIR is more appropriate than FTIR-RAS and FTIR-SEIRAS regarding fuel cells devices operating with ethanol.

2. EXPERIMENTAL

2.1 Electrodes Preparation

Four electrodes were prepared with Pt/C Etek[®] 20% in metal loading in three different supports: i) First, a Pt/C on Au support (0.78 cm²) was prepared. The catalyst was dispersed in ultrapure water (2 mg mL⁻¹) and sonicated for 60 minutes. Next, 20 μL of the dispersed suspension was added on the substrate surface and dried in air. ii) A Pt/C with 5% Nafion solution (Aldrich) on Au support (0.78 cm²) was prepared, as described in iii. iii) A Pt/C with 5% Nafion solution on glass carbon support (0.071 cm²) was prepared. The dispersion for each of these two electrodes was prepared in ultrapure water (1 mg mL⁻¹) with a 5% Nafion solution in a ratio of 1:100 v/v, and the powder was ultrasonically dispersed in ultrapure water for 60 min. A 20-μL aliquot of the dispersed suspension was subsequently added in a Au support and 4 μL in a glass carbon support, and each was dried in air. iv) A Pt/C with Nafion on a Teflon treated carbon cloth (Electroche, inc.) (0.8 cm²) was prepared as a MEA, as described by De Souza *et al.* [1].

2.2 Electrochemical and Spectroelectrochemical Experiments

Electrochemical experiments were performed using an Autolab PGSTAT 302N potentiostat. The preparation of the electrodes used in these experiments was described above. A Pt sheet (A = 2 cm²) and a reversible hydrogen electrode were used as counter and reference electrodes, respectively. The cyclic voltammetric experiments were performed in a 0.1 mol L⁻¹ HClO₄ solution in the absence and in the presence of ethanol. Before each experiment, the electrochemical cell was purged for 15 min with N₂.

The spectroelectrochemical ATR-FTIR *in situ* measurements were carried out using a Varian[®] 660 IR spectrometer equipped with a MCT detector cooled with liquid N₂, a MIRacle with a Diamond/ZnSe Crystal Plate (Pike [®]) ATR accessory and a special cell as presented in the literature [32].

The same working electrodes used in the electrochemical experiments were used in ATR-FTIR measurements. These experiments were performed at 25 °C in a 0.1 mol L⁻¹ HClO₄ containing 2.0 mol L⁻¹ ethanol. The spectra were collected as the ratio R:R₀, where R represents a spectrum at a given potential, and R₀ is the spectrum collected at 0.05 V. Positive and negative directional bands represent gains and losses of species at the sampling potential, respectively. The spectra were computed from 96 interferograms averaged from 2500 cm⁻¹ to 850 cm⁻¹ with the spectral resolution set to 8 cm⁻¹. Initially, a reference spectrum, R₀, was measured at 0.05 V, and sample spectra were collected after applying successive potential steps from 0.2 V to 0.8 V.

3. RESULTS AND DISCUSSION

Figure 1 shows the cyclic voltammograms of the electrochemical characterization of the Pt/C electrodes that were mentioned previously. In electrodes that are supported on Au or glass carbon, the typical profile of Pt/C in an acid medium is well-defined, with the regions of adsorption/desorption of hydrogen (between 0.05 and 0.4 V) and oxidation/reduction of the PtO (between 0.8 and 1.2 V) being in accordance with the literature for Pt/C [33-35].

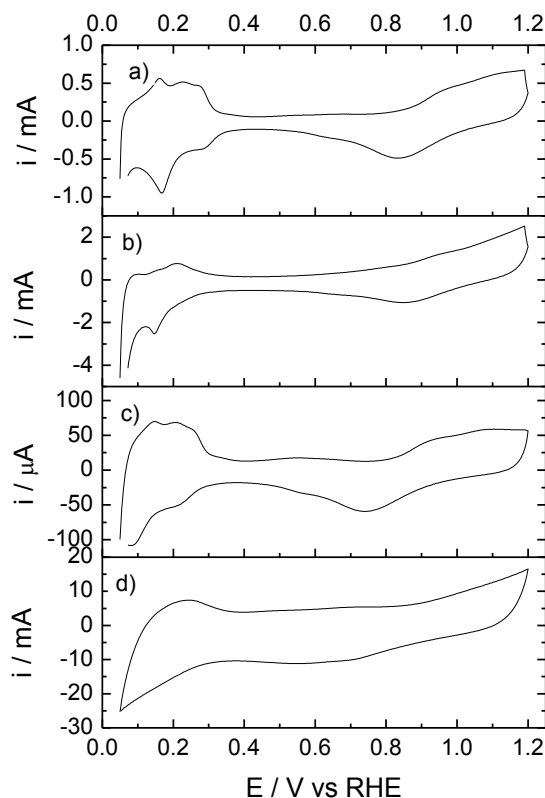


Figure 1. Cyclic voltammograms of a) Pt_{Etek}/C without Nafion on Au support, b) Pt_{Etek}/C with Nafion on Au support, c) Pt_{Etek}/C with Nafion on glass carbon support, and d) Pt_{Etek}/C on Teflon treated carbon cloth in 0.1 mol L⁻¹ HClO₄ aqueous solutions at a potential sweep rate of 50 mV s⁻¹. T = 25 °C.

However, in the electrode supported on Teflon treated carbon cloth, the hydrogen peaks of the Pt polycrystalline are not well-defined and are more resistive than the other electrodes studied. This profile is similar to that which was obtained by Lizcano-Valbuena *et al.* [23] using a Pt/C Etek® on work describing a gas diffusion electrode in a electrochemical experiments. One explanation for this behavior could be that there are features of the carbon support that mask the hydrogen desorption characteristics of Pt [36, 37].

Table I presents data about the surface area of Pt and the roughness factor (RF) for each electrode. These values were obtained using the cyclic voltammetry data to calculate the surface area of the Pt electrode with an established procedure [38, 39]. This procedure considers a charge density of 210 $\mu\text{C cm}^{-2}$ to be equivalent to the desorption of one hydrogen monolayer on Pt. The RF of the Teflon-treated carbon cloth is approximately one order of magnitude larger than the other electrodes. This observation is expected due to the high surface area of the carbon cloth.

Table I: Electroactive surface areas and roughness factor of the different electrodes.

Electrode	Pt _{Etek} /C without Nafion on Au support	Pt _{Etek} /C with Nafion on Au support	Pt _{Etek} /C with Nafion on glass carbon support	Pt _{Etek} /C on carbon cloth Teflon treated
Platinum Area / cm^2	8	4	1	171
AES* / $\text{m}^2 \text{g}^{-1}$	102	44	55	21
DU(Pt)** / %	43	19	23	9
Roughness factor	10	5	12	214

* Electrochemically accessible surface area

** degree of utilization of Pt (surface Pt atoms / total Pt atoms)

Other possible data obtained with these experiments are the electrochemically accessible surface (AES), the Pt loading is an important parameter, not only because it establishes the cost, but because it should be the same in order to effectively compare different preparation procedures of supported Pt/C electrodes by cyclic voltammetry [40].

All electrodes containing Nafion had their AES measured less than Pt_{Etek}/C without Nafion on Au support, this can be attributed by the loss of surface area on the Nafion impregnated Pt/C catalyst to the blocking of the Pt sites and to the inaccessibility of the protons to the Pt surfaces which are present between the Pt crystallites and the carbon support [41]. However, Pt_{Etek}/C on carbon cloth Teflon treated that even with their greater surface area its AES is the lowest of all areas measured, indicating a low dispersion of the electrocatalysts on the support, confirmed by the degree of utilization of platinum for the electrodes.

Figure 2 shows the results of the linear sweep voltamogrammetries at 10 mV s^{-1} obtained for all electrodes at 2 mol L^{-1} of ethanol concentration. Of note is that the onset potential for the EOR on the Pt/C Etek electrodes supported in Au and GC is about 0.35 V. The current densities for ethanol oxidation for these electrodes are greater than those observed for the same process on Pt/C Etek

supported on Teflon treated carbon cloth; however, the onset potential for the same reaction in this electrode is approximately 70 mV lower than the one for the other electrodes. Additionally, the Pt/C Etek supported on Au has higher current densities than the Pt/C Etek supported on carbons. These features show that the activity is not only dependent of roughness, or dispersion of platinum nanoparticles, but also on the nature of the support.

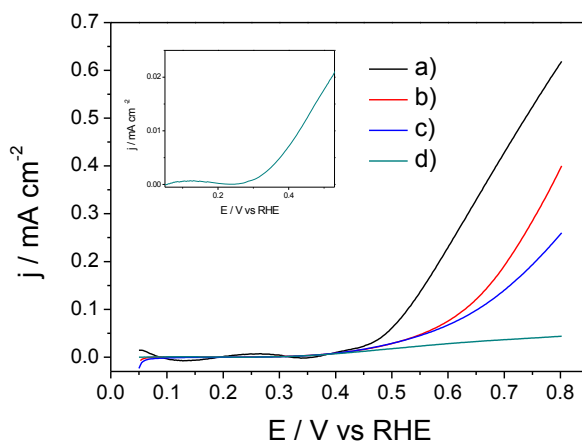


Figure 2. Linear sweep voltammograms of a) Pt_{Etek}/C without Nafion on Au support, b) Pt_{Etek}/C with Nafion on Au support, c) Pt_{Etek}/C with Nafion on glass carbon support, and d) Pt_{Etek}/C on carbon cloth Teflon treated in 2.0 mol L⁻¹ CH₃CH₂OH + 0.1 mol L⁻¹ HClO₄ aqueous solutions at a potential sweep rate of 10 mV s⁻¹. In the inset there is the onset potential of the Pt_{Etek}/C on carbon cloth Teflon treated. T = 25 °C

Park and Popov [22] studied the difference in performance between carbon cloth and carbon paper in a GDL electrode. These researchers indicated that the factors that influence performance in a single fuel cell are electrical resistance, hydrophobicity, and diffusion of the reactants of the GDL, thereby causing a change in the conditions of charge-transfer resistance [42]. For this reason, the results outlined above for the ethanol oxidation can be explained by considering the lower current densities for the process of Pt/C Etek on carbon cloth due to hydrophobicity and diffusion, thereby resulting in a high charge transfer-resistance.

The effect of the support has also been explained in the literature in electrochemical experiments. Suffredini *et al.* [43], using Pt–RuO₂/C supported on boron-doped diamond (DDB) and on glassy carbon, reported that DDB present lower capacity currents and promoted a better distribution of the powder on their surface. These factors were found to influence electrocatalytic activity for methanol and ethanol oxidation.

To understand the differences in the activity of ethanol oxidation on the different electrodes, insight into the products generated is necessary. To accomplish this understanding, all of the electrodes were tested in experiments using the *in situ* ATR-FTIR, in ethanol 2.0 mol L⁻¹ and 0.1 mol L⁻¹ HClO₄.

Figure 3 shows one set of spectra that was measured for ethanol oxidation for each electrode at ethanol 2 mol L⁻¹. Bands corresponding to acetic acid (1280 cm⁻¹) [44], acetaldehyde (933 cm⁻¹) [45] and CO₂ (2343 cm⁻¹) [10] were measured. Additionally, three other spectral bands can be observed at 1130, ~1630 and 1710 cm⁻¹, these bands may be ascribed to the triply

degenerate ν_3 mode of adsorbed perchlorate anions, the HOH deformation, and the C=O stretch of the carbonyl group, respectively [46].

The FTIR spectra obtained for all electrodes suggested that different supports do not provoke the occurrence of additional pathways of oxidation, thereby producing CO_2 , acetic acid, and acetaldehyde. However, the potential of appearance of the bands are different for each electrode.

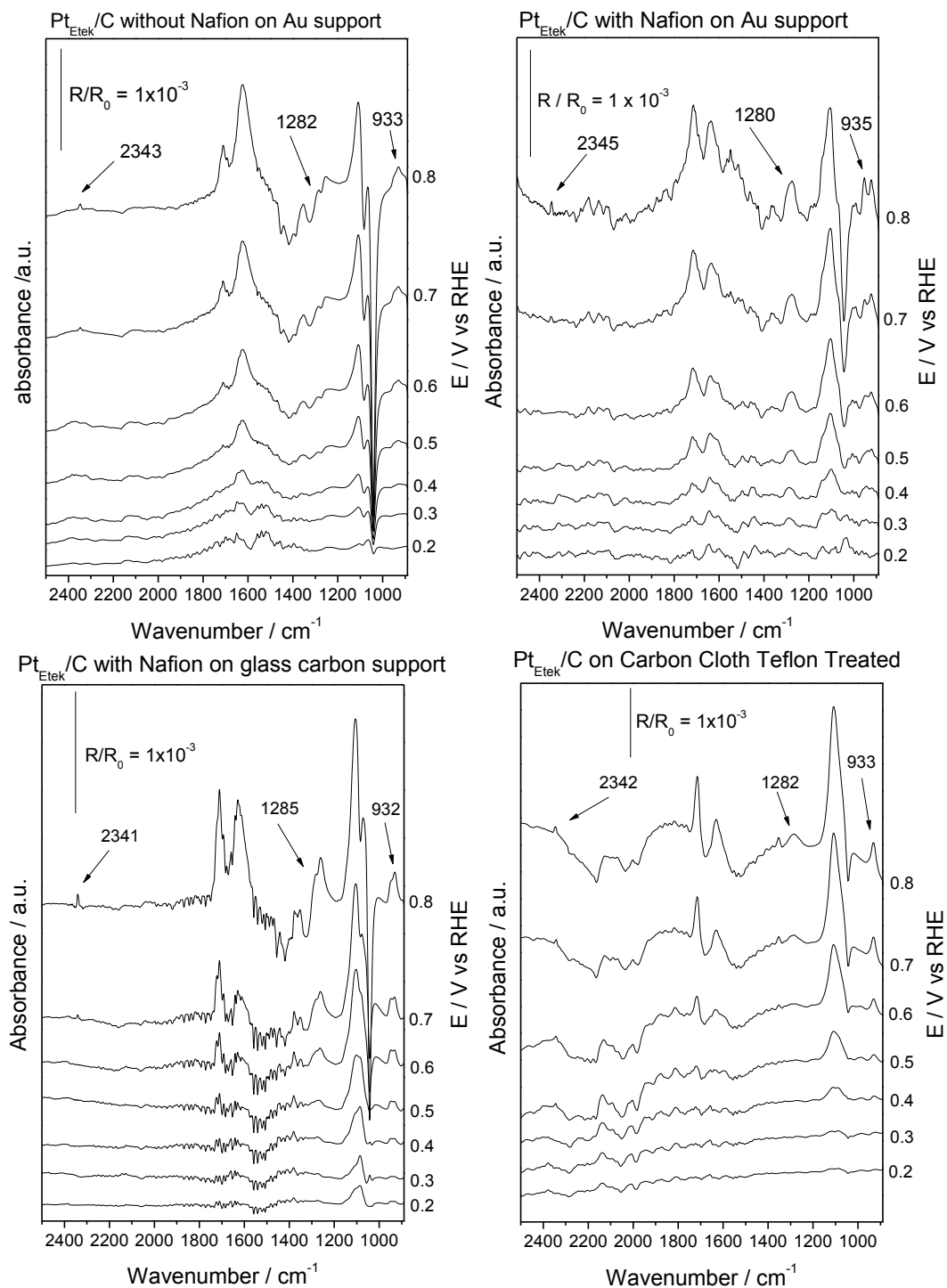


Figure 3. *In situ* FTIR spectra collected at several potentials for EOR on all Pt electrodes. Backgrounds collected at 0.05 V (RHE scale).

To evaluate the effect of catalyst support on the product distribution during the EOR at different potentials, all bands were deconvoluted to Lorentzian line forms [32], and normalized using the band intensities at all potentials divided by the band intensity obtained at 0.8V for each electrode [47]. Thus, the intensity and line width of each band could be individually analyzed. Figure 4 presents the normalized intensities of the acetic acid, acetaldehyde and CO₂.

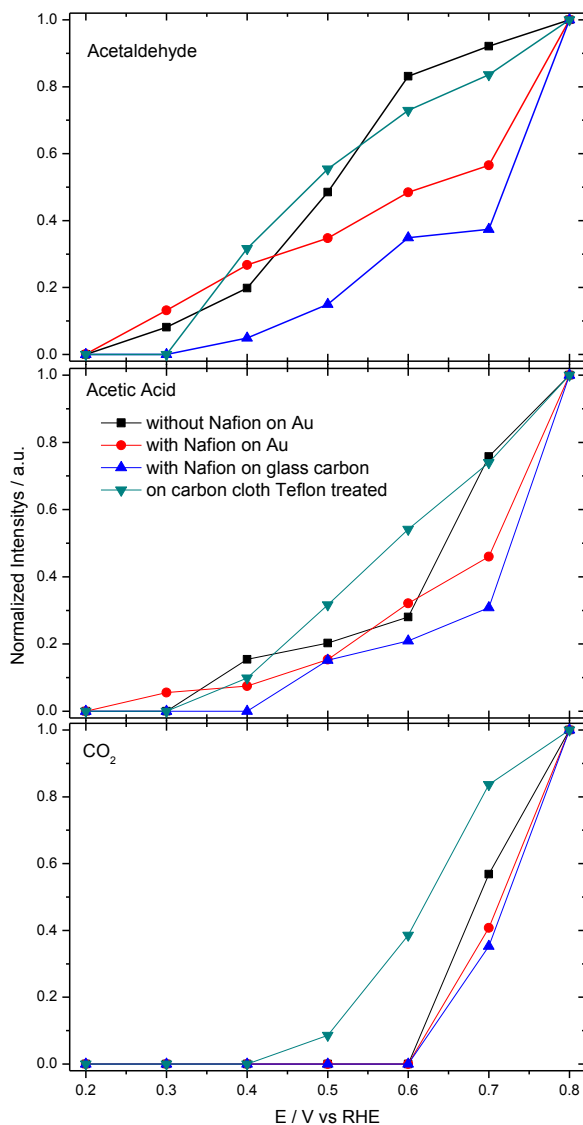


Figure 4. Acetaldehyde, Acetic Acid and CO₂ band intensities as a function of the potential for Pt_{Etek}/C without Nafion on Au support, Pt_{Etek}/C with Nafion on Au support, Pt_{Etek}/C with Nafion on glass carbon support, and Pt_{Etek}/C on carbon cloth Teflon treated. Data extracted from Fig. 3.

For the EOR on carbon cloth electrode the CO₂ bands appear in 0.5 V vs RHE, which means 0.2 V smaller than CO₂ bands appear for the other electrodes. This fact can be interpreted in terms of a higher capability of rough electrodes to interact with adsorbed ethanol molecules, thus facilitating the

scission of the carbon chain that ultimately produces CO_2 as oxidation product. It is in agreement with reported by Giz *et al.*[48] in which roughness PtRu electrodeposits are selective to the pathway towards the formation of CO_2 . Additionally, Qian *et al.* [49] studied platinum electrodeposited on gold for ethanol oxidation reported that CO_2 formation increases with the increase of surface roughness of the Pt film.

To assess a comparative relationship between the electrocatalysts studied, the integrated band intensities for the CO_2 /acetaldehyde and the CO_2 /acetic acid ratios as a function of the electrode potential have been examined. Those results are presented in Figure 5.

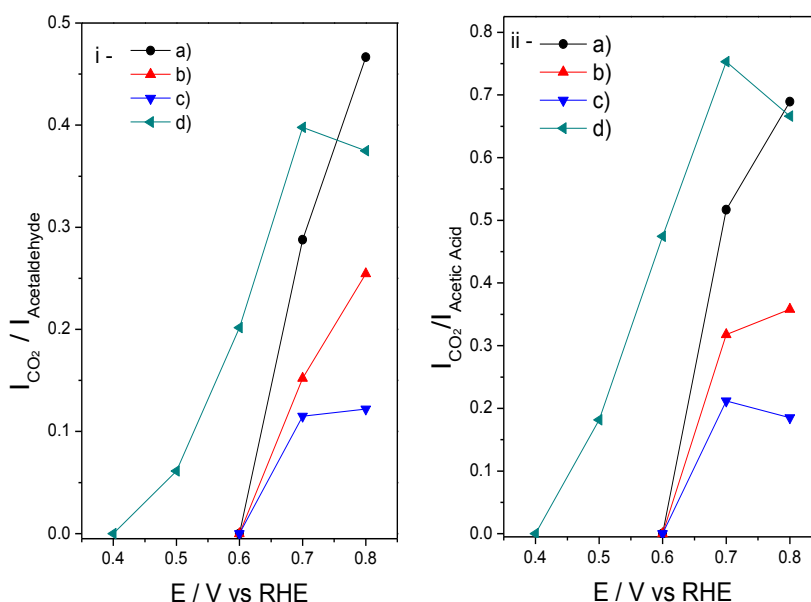


Figure 5. Band intensities ratios of i) CO_2 /acetaldehyde, ii) CO_2 /acetic acid on the a) $\text{Pt}_{\text{Etek}}/\text{C}$ without Nafion on Au support, b) $\text{Pt}_{\text{Etek}}/\text{C}$ with Nafion on Au support, c) $\text{Pt}_{\text{Etek}}/\text{C}$ with Nafion on glassy carbon support, and d) $\text{Pt}_{\text{Etek}}/\text{C}$ on carbon cloth Teflon treated as a function of the electrode potential in $2 \text{ mol L}^{-1} \text{ C}_2\text{H}_5\text{OH} + 0.1 \text{ mol L}^{-1} \text{ HClO}_4$ aqueous solution.

The ratio bands of CO_2 and acetaldehyde are presented in Figure 7i. In all of the electrodes, the production of acetaldehyde is favored. This fact is in agreement with reports by Camara and Iwasita [10]. With high ethanol concentration, there is a decrease in the formation of products that require oxygen (namely, CO_2 and acetic acid), while the acetaldehyde production is still favored.

Considering the ratio bands of CO_2 and acetic acid, there is a small influence of acetic acid production for all electrodes. However, the most important feature revealed by figure 7i e 7ii as we have already discussed above in Figure 4, is that CO_2 is produced in a greater amount from ethanol oxidation from Pt/C Etek supported on carbon cloth compared to the CO_2 amounts produced using the other electrodes. This behavior is uncommon in the literature, and it is only able to be measured due to the configuration of the *in situ* ATR-FTIR setup developed using Teflon-treated carbon cloth.

To summarize the results obtained here there are some evidences regarding the utilization

of Pt_{Etek}/C on Carbon cloth teflon treated electrode for ethanol oxidation: i) the lowest onset potential; ii) production of CO₂ at lowest potentials; iii) the highest roughness, iv) the lowest dispersion of Pt and v) the highest hydrophobicity.

4. CONCLUSIONS

PtEtek/C presented different activity for the ethanol oxidation reaction depending on the support. This difference can be explained by hydrophobicity, diffusion, roughness, dispersion, and /or charge transfer-resistance intrinsic for each support material. When studied Pt/C on carbon cloth was seen that support facilitates the C-C bond cleavage. Of note is the cleavage at high ethanol concentrations. The new ATR-FTIR setup demonstrated a powerful technique for studies in non-reflective and rough electrodes.

ACKNOWLEDGMENTS

The authors wish to thank the Brazilian Funding Institutions (CAPES, CNPq 473308/2010-0, FAPESP (Processes Numbers: 09/09145-6, 10/07831-7, 10/03037-4, 10/16511-6), INCT (Process Number: 573.783/2008-0) and UFABC for their financial support.

References

1. R.F.B. De Souza, L.S. Parreira, D.C. Rascio, J.C.M. Silva, E. Teixeira-Neto, M.L. Calegari, E.V. Spinace, A.O. Neto, M.C. Santos, *J. Power Sources*. 195 (2010) 1589.
2. R.F.B. De Souza, M.M. Tusi, M. Brandalise, R.R. Dias, M. Linardi, E.V. Spinace, M.C. dos Santos, A.O. Neto, *Int. J. Electrochem. Sci.* 5 (2010) 895.
3. F.C. Simões, D.M. dos Anjos, F. Vigier, J.M. Léger, F. Hahn, C. Coutanceau, E.R. Gonzalez, G. Tremiliosi-Filho, A.R. de Andrade, P. Olivi, K.B. Kokoh, *J. Power Sources*. 167 (2007) 1.
4. A.O. Neto, M. Linardi, D.M. dos Anjos, G. Tremiliosi, E.V. Spinace, *J. Appl. Electrochem.* 39 (2009) 1153.
5. T. Iwasita, E. Pastor, *Electrochim. Acta.* 39 (1994) 531.
6. J.F. Gomes, B. Busson, A. Tadjeddine, G. Tremiliosi-Filho, *Electrochim. Acta.* 53 (2008) 6899.
7. V. Pacheco Santos, V. Del Colle, R.B. de Lima, G. Tremiliosi-Filho, *Electrochim. Acta.* 52 (2007) 2376.
8. B. Rasch, T. Iwasita, *Electrochim. Acta.* 35 (1990) 989.
9. T. Iwasita, G.A. Camara, in: S. Shi-Gang, C. Paul Andrew, W. Andrzej (Eds.), *In-situ Spectroscopic Studies of Adsorption at the Electrode and Electrocatalysis*, Elsevier Science B.V., Amsterdam, 2007, pp. 33-61.
10. G.A. Camara, T. Iwasita, *J. Electroanal. Chem.* 578 (2005) 315.
11. T. Iwasita, *Electrochim. Acta.* 47 (2002) 3663.
12. S.-G. Sun, Y. Lin, *Electrochim. Acta.* 44 (1998) 1153.
13. N.M. Markovic, H.A. Gasteiger, P.N. Ross, X. Jiang, I. Villegas, M.J. Weaver, *Electrochim. Acta.* 40 (1995) 91.
14. G.A. Camara, J.F. Gomes, K. Bergamaski, E. Teixeira-Neto, F.C. Nart, *J. Electroanal. Chem.* 617 (2008) 171.
15. F. Vigier, C. Coutanceau, F. Hahn, E.M. Belgsir, C. Lamy, *J. Electroanal. Chem.* 563 (2004) 81.

16. R.F.B. De Souza, L.S. Parreira, J.C.M. Silva, F.C. Simões, M.L. Calegaro, M.J. Giz, G.A. Camara, A.O. Neto, M.C. Santos, *Int. J. Hydrogen Energy*. 36 (2011) 11519.
17. Y.X. Chen, S. Ye, M. Heinen, Z. Jusys, M. Osawa, R.J. Behm, *J. Phys. Chem. B*. 110 (2006) 9534.
18. T. Sato, K. Kunitatsu, H. Uchida, M. Watanabe, *Electrochim. Acta*. 53 (2007) 1265.
19. H. Miyake, S. Ye, M. Osawa, *Electrochem. Comm.* 4 (2002) 973.
20. A. Miki, S. Ye, T. Senzaki, M. Osawa, *J. Electroanal. Chem.* 563 (2004) 23.
21. S. Park, B.N. Popov, *Fuel*. 88 (2009) 2068.
22. S. Park, B.N. Popov, *Fuel*. 90 (2011) 436.
23. W.H. Lizcano-Valbuena, V.A. Paganin, E.R. Gonzalez, *Electrochim. Acta*. 47 (2002) 3715.
24. V.A. Paganin, E.A. Ticianelli, E.R. Gonzalez, *J. Appl. Electrochem.* 26 (1996) 297.
25. A.R. Hind, S.K. Bhargava, A. McKinnon, *Adv. Colloid Interface Sci.* 93 (2001) 91.
26. U.P. Fringeli, in: L. John (Ed.), *Encyclopedia of Spectroscopy and Spectrometry*, Academic Press, Oxford, 1999, pp. 94.
27. M.H.M.T. Assumpção, R.F.B. De Souza, D.C. Rascio, J.C.M. Silva, M.L. Calegaro, I. Gaubeur, T.R.L.C. Paixão, P. Hammer, M.R.V. Lanza, M.C. Santos, *Carbon*. 49 (2011) 2842.
28. S.D. Ebbesen, B.L. Mojet, L. Lefferts, *J. Catal.* 246 (2007) 66.
29. Z. Wang, M. Grahn, M.L. Larsson, A. Holmgren, J. Sterte, J. Hedlund, *Sensors and Actuators B*. 115 (2006) 685.
30. W. Liao, F. Wei, D. Liu, M.X. Qian, G. Yuan, X.S. Zhao, *Sensors and Actuators B*. 114 (2006) 445.
31. J. Schmitt, D. Nivens, D.C. White, H.-C. Flemming, *Water Science and Technology*. 32 (1995) 149.
32. J.C.M. Silva, L.S. Parreira, R.F.B. De Souza, M.L. Calegaro, E.V. Spinacé, A.O. Neto, M.C. Santos, *Appl. Catal. B*. 110 (2011) 141.
33. E.V. Spinacé, A.O. Neto, T.R.R. Vasconcelos, M. Linardi, *J. Power Sources*. 137 (2004) 17-.
34. J.C.M. Silva, R.F.B. De Souza, L.S. Parreira, E.T. Neto, M.L. Calegaro, M.C. Santos, *Appl. Catal. B*. 99 (2010) 265.
35. L. Colmenares, H. Wang, Z. Jusys, L. Jiang, S. Yan, G.Q. Sun, R.J. Behm, *Electrochim. Acta*. 52 (2006) 221.
36. U. Koponen, H. Kumpulainen, M. Bergelin, J. Keskinen, T. Peltonen, M. Valkiainen, M. Wasberg, *J. Power Sources*. 118 (2003) 325.
37. S. Srinivasan, E.A. Ticianelli, C.R. Derouin, A. Redondo, *J. Power Sources*. 22 (1988) 359.
38. S. Trasatti, A. Petrii, *Pur. Appl. Chem.* 63 (1991) 71.
39. R.F.B. De Souza, A.E.A. Flausino, D.C. Rascio, R.T.S. Oliveira, E.T. Neto, M.L. Calegaro, M.C. Santos, *Appl. Catal. B*. 91 (2009) 516.
40. A. Pozio, M. De Francesco, A. Cemmi, F. Cardellini, L. Giorgi, *J. Power Sources*. 105 (2002) 13.
41. G. Tamizhmani, J.P. Dodelet, D. Guay, *J. Electrochem. Soc.* 143 (1996) 18.
42. A.Z. Weber, J. Newman, *J. Electrochem. Soc.* 152 (2005) A677.
43. H.B. Suffredini, V. Tricoli, N. Vatistas, L.A. Avaca, *J. Power Sources*. 158 (2006) 124.
44. J.M. Léger, S. Rousseau, C. Coutanceau, F. Hahn, C. Lamy, *Electrochim. Acta*. 50 (2005) 5118.
45. M. Li, A. Kowal, K. Sasaki, N. Marinkovic, D. Su, E. Korach, P. Liu, R.R. Adzic, *Electrochim. Acta*. 55 (2010) 4331.
46. S.C.S. Lai, S.E.F. Kleijn, F.T.Z. Öztürk, V.C. van Rees Vellinga, J. Koning, P. Rodriguez, M.T.M. Koper, *Catal. Today*. 154 (2010) 92.
47. M.J. Giz, G.A. Camara, *J. Electroanal. Chem.* 625 (2009) 117.
48. M.J. Giz, G.A. Camara, G. Maia, *Electrochem. Comm.* 11 (2009) 1586.
49. Q.-Y. Qian, C. Yang, Y.-G. Zhou, S. Yang, X.-H. Xia, *J. Electroanal. Chem.* 660 (2011) 57